Supporting Information for:

Ratiometric Zinc Sensing by Time-Resolved Fluorescence Spectroscopy.

Maksim Royzen, Alexander Durandin, Victor G. Young, Jr.,[†] Nicholas E. Geacintov,*
James W. Canary*

Department of Chemistry, New York University, New York, NY 10003
University of Minnesota, 207 Pleasant St., S.E., Minneapolis, MN 55455

Contents:

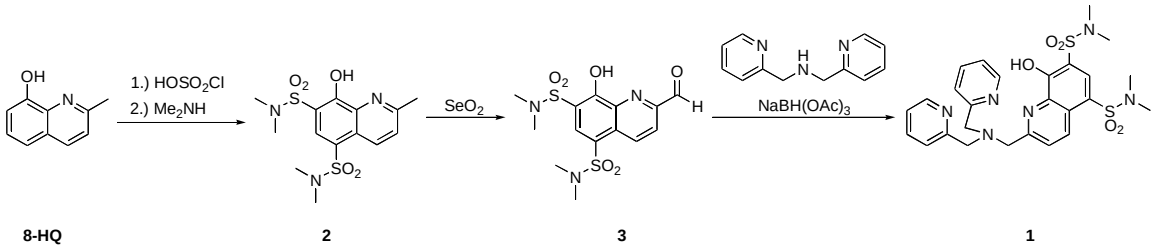

Scheme S1. Synthesis of **1**.

8-Hydroxy-2-methyl-quinoline-5,7-bis(N,N-dimethyl)sulfonamide (2)
Compound **2** was previously reported. It was synthesized according to the literature method.[i]

8-Hydroxyquinoline-5,7-bis(N,N-dimethyl)sulfonamide-2-carbaldehyde (3)
Under dry conditions anhydrous 1,4-dioxane (80 mL) was added to **2** (2.7 g, 8.71 mmol), SeO2 (0.967 g, 8.71 mmol), and molecular sieves (8 g). The resulting mixture was refluxed at 90 °C under argon atmosphere for 5 days. After that, the mixture was cooled down to room temperature and filtered through a pad of Celite. The Celite was rinsed with 1,4-dioxane (80 mL) and the solvent was evaporated under reduced pressure. The crude product was redissolved in methylene chloride (200 mL), washed with brine (50 mL) and water (50 mL), and dried with Na_2SO_4. Upon evaporating the solvent, the product was carried over to the next step without further purification. Yield = 2.1 g (75%). ^{1}H NMR ($CDCl_3$) δ 10.20 (s, 1H), 9.25 (d, J = 8.8, 1H), 8.57 (s, 1H), 8.25 (d, J = 8.8, 1H), 2.90 (s, 6H), 2.79 (s, 6H). MS (Maldi-TOF) Calc. (M + H^+) 388.06, Found 388.25.

Bis(2-pyridylmethyl)(8-Hydroxyquinoline-5,7-bis(N,N,-dimethyl)sulfonamide-2-methyl)amine (1)
Methylene chloride (10 mL) was added to a mixture containing **2** (0.154 g, 0.398 mmol), sodium triacetoxyborohydride (0.127 g 0.597 mmol), and dipycolylamine (39.6 mg, 0.199 mmol). The reaction mixture was stirred overnight at room temperature. The product mixture was diluted with methylene chloride (90 mL) and was extracted with 10 M HCl (20 mL). The aqueous layer was neutralized with NaOH and the product was extracted with methylene chloride (100 mL). Yield = 0.180 g (81%). ^{1}H NMR ($CDCl_3$) δ 9.02 (d, J = 8.7, 1H), 8.64 (d, J = 4.1, 2H), 8.56 (s, 1H), 7.72 (t, J = 7.6, 2H), 7.67 (d, J = 8.9, 1H), 7.51 (d, J = 7.7, 2H), 7.23 (t, J = 5.1, 2H), 4.14 (s, 2H), 4.01 (s, 4H), 3.00 (s, 6H), 2.82 (s, 6H). ^{13}C NMR ($CDCl_3$) δ 158.36, 157.91, 157.55, 149.18, 138.73, 136.86, 134.88, 131.76, 126.15, 124.79, 123.92, 122.56, 121.26, 118.34, 59.44, 57.70, 37.88, 37.52. MS (Maldi-TOF) Calc. 571.17 (M + H^+), Found 570.51. Anal. Calc. for $C_{27}H_{35}N_6NaO_7S_2$ (**M** + NaOH, MeOH): C, 50.46; H, 5.49; N, 13.08. Found: C, 50.66; H, 5.34; N, 13.29.

[Zn(1)]
(**Caution!** *Perchlorate salts of metal complexes with organic ligands are potentially explosive. They should be handled in small quantity and with caution.)* Zn^{2+} complex of **1** was formed by combining equimolar quantities of $Zn(ClO_4)_2$, **1** and NaOH. Aqueous stock solution containing 0.02 M $Zn(ClO_4)_2$ (0.875 mL) was added to **1** (10 mg, 0.0175 mmol) dissolved in acetonitrile. To this solution NaOH (0.7 mg, 0.0175 mmol) dissolved in water (0.1 mL) was added. Upon concentrating the solvent, yellow precipitate formed. Yellow powder was filtered out and dried

under vacuum. ^{1}H NMR (CD_3OD) δ 9.02 (d, J = 8.8, 1H), 8.74 (d, J = 4.8, 2H), 8.43 (s, 1H), 8.09 (t, J = 1.6, 2H), 7.65 (m, 5H), 4.55 (d, J = 5.1, 4H), 4.39 (s, 2H), 3.01 (s, 6H), 2.68 (s, 6H). ESI-MS Calc. 633.09 (M^+), Found 633.2.

[1] Pearce, D. A.; Jotterand, N.; Carrico, I. S.; Imperiali, B. *J. Am. Chem. Soc.* **2001**, *123*, 5160.

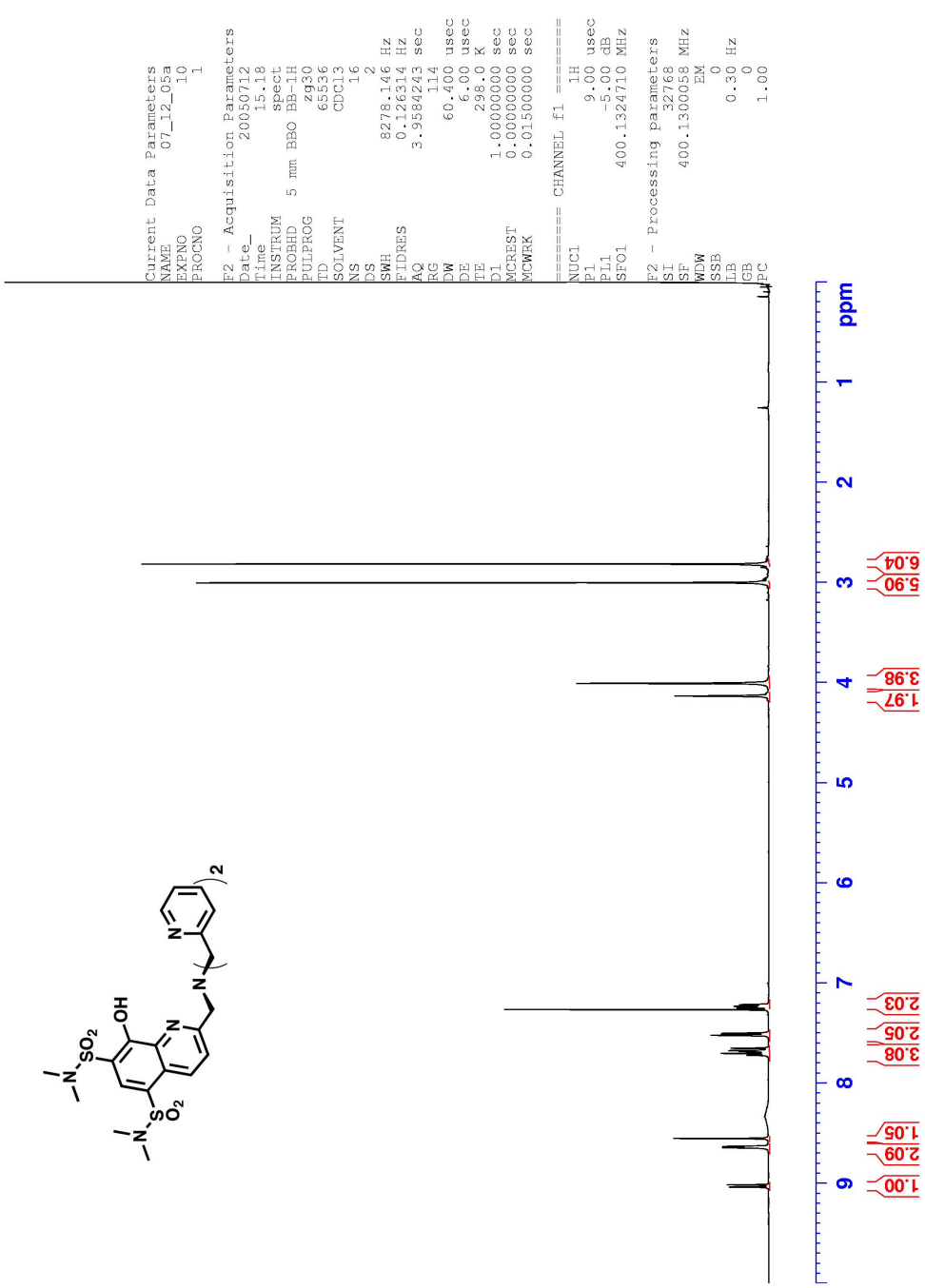

Figure S1. ^{1}H NMR spectrum of **1**.

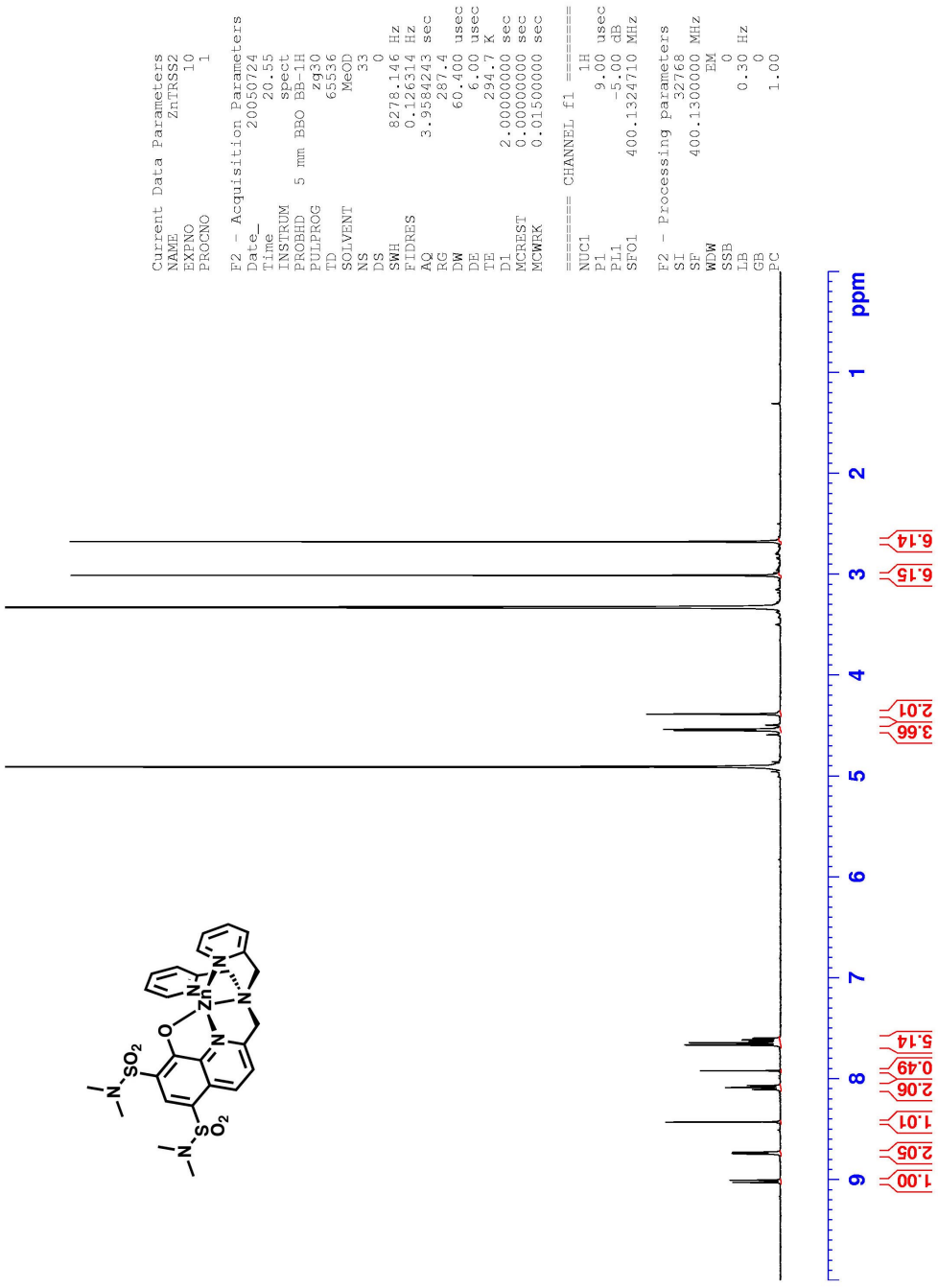

Figure S2. ^{1}H NMR spectrum of [Zn(**1**)].

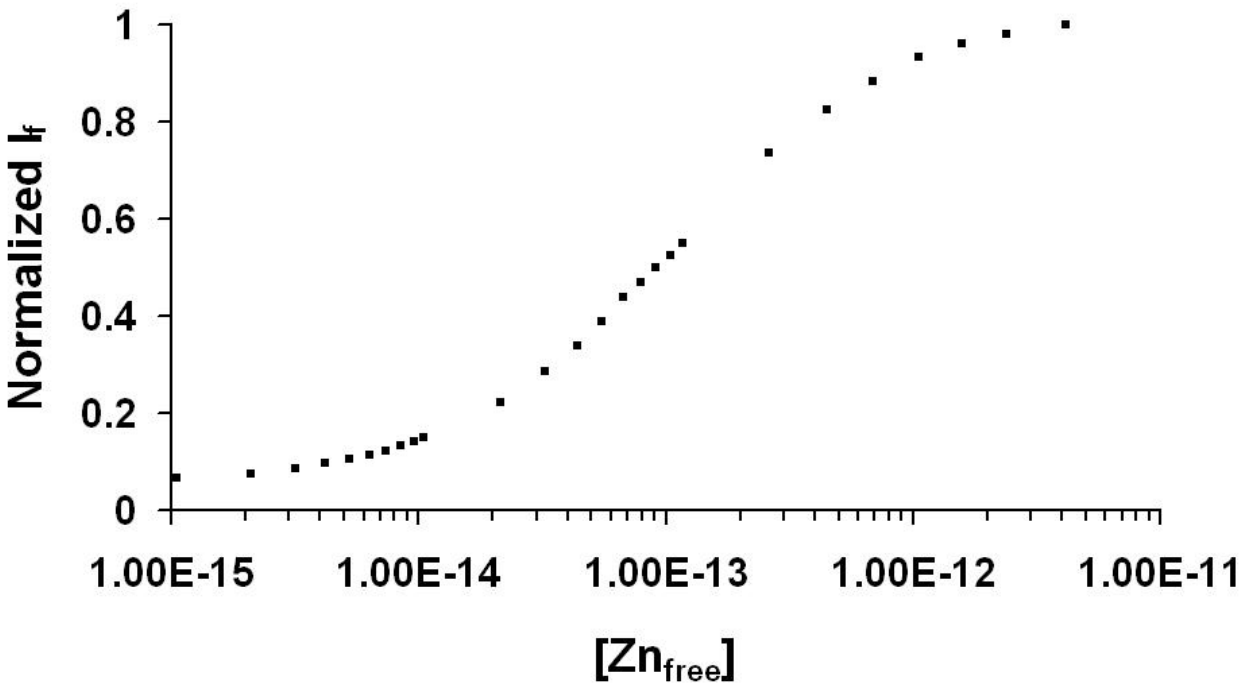

Figure S3. Fluorescence response of **1** (10 μM) to buffered Zn^{2+} solutions. Spectra were acquired in aqueous solutions (0.1 M KNO_3, 50 mM HEPES, pH 7.2, 25 ^oC) with excitation at 340 nm. Zinc ion concentration was buffered by 10 mM HEDTA. The spectra shown are for total Zn^{2+} at 0.01, 0.02, 0.03, 0.04, 0.05, 0.06, 0.07, 0.08, 0.09, 0.1, 0.2, 0.3, 0.4, 0.5, 0.6, 0.7, 0.9, 1, 2, 3, 4, 5, 6, 7, 8 mM with corresponding free Zn^{2+} at $10^{-14.98}$, $10^{-14.68}$, $10^{-14.5}$, $10^{-14.38}$, $10^{-14.28}$, $10^{-14.2}$, $10^{-14.132}$, $10^{-14.07}$, $10^{-14.02}$, $10^{-13.98}$, $10^{-13.67}$, $10^{-13.49}$, $10^{-13.36}$, $10^{-13.26}$, $10^{-13.17}$, $10^{-13.1}$, $10^{-13.04}$, $10^{-12.98}$, $10^{-12.93}$, $10^{-12.58}$, $10^{-12.35}$, $10^{-12.16}$, $10^{-11.98}$, $10^{-11.80}$, $10^{-11.62}$, $10^{-11.38}$ M, respectively.

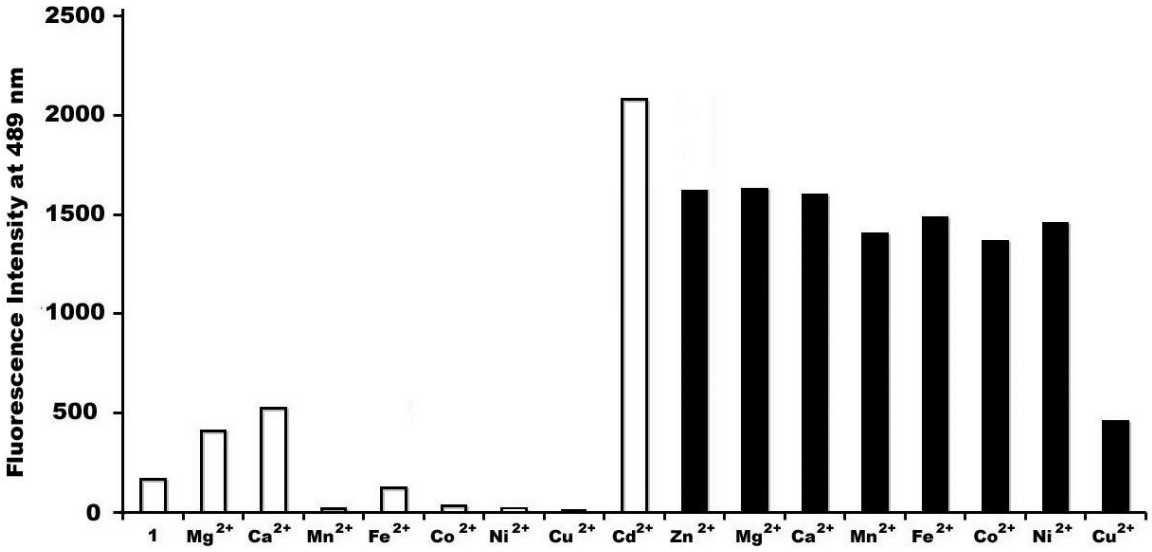

Figure S4. Fluorescence response of **1** to first row transition metal ions in the absence of Zn^{2+} (□) and in the presence of Zn^{2+} (■).

Equivalents of Zn^{2+} added	τ_f (ns)	A_f (%)	τ_{Zn} (ns)	A_{Zn} (%)	χ^2
0	0.640	95.6	24.9	4.4	1.18
0.1	0.633	88.3	24.4	11.7	1.09
0.2	0.609	81.0	24.1	19.0	1.01
0.3	0.629	72.2	23.7	27.8	0.08
0.4	0.615	63.6	23.4	36.4	0.99
0.5	0.626	54.2	23.2	45.8	1.01
0.6	0.595	44.2	22.8	55.8	0.94
0.7	0.711	31.2	22.9	68.8	1.01
0.8	0.620	20.9	22.6	79.1	1.04
0.9	1.082	7.9	22.4	92.1	1.02
1	—	0	22.5	100	1.0
1.2	—	0	22.4	100	1.03
Average	0.676		23.3		

Table S1. Fluorescence lifetime constants of the two decay components observed when performing TRFS titration of 1 μM of **1** with $Zn(ClO_4)_2$ in aqueous buffer solution (0.1 M KNO_3, 50 mM HEPES, pH 7.0, 25 ^oC).

TRFS studies were carried out using FluoTime photon counting electronics (TimeHarp 200, Picoquant Gmbh) and Hamamatsu H5783P PMT, which made it possible to achieve resolution of decay times down to 35 picoseconds after deconvolution. The system works in the reversed start-stop mode, allowing operating up to 80 MHz repetition rate and count rates up to 3 Mcounts per second can be processed. We used count rate not more than 10 Kcount per second to obtain the best time resolution of the system. As a source of excitation we used femtosecond TiSp laser (Coherent MIRA 900) with the Argon Ion laser (Coherent Innova310) as a pump source. Mira 900 laser has a pulse width ~120 fs and is much shorter than the response time of the registration system. In order to obtain the best resolution in our time domain the repetition

rate of the laser pulses was divided typicalli 8 times to 1 MHz with the CONOPTICS Model 305 Syncronous countdown and Model 25D driver of the divider system. Phillips Scientific wideband amplifier (Model 6954) was used to amplify and normalize syncronization pulses from Mira 900 laser.

Mira 900 has a wavelength range of 700 – 1000 nm which is typical for TiSp laser and U – Oplaz femtosecond second and third harmonic generator was used to provide excitation in the UV – part of spectrum.

To optimize intensity and spectral resolution of the photoemission high resolution spectrograph “AriesFF250 was used in the registration arm of the spectrometer.
All data acquisition functions of the FluoTime spectrometer are controlled by software for Windows. The software provides functions such as setup of parameters and control of the measurement in the selected operation mode. FluoFit software (also by Picoquant Gmbh) was used for deconvolution of decays and further analysis of the experimental data.

Concentration dependence of the fluorescence characteristics of 1 in the absence of Zn(II).

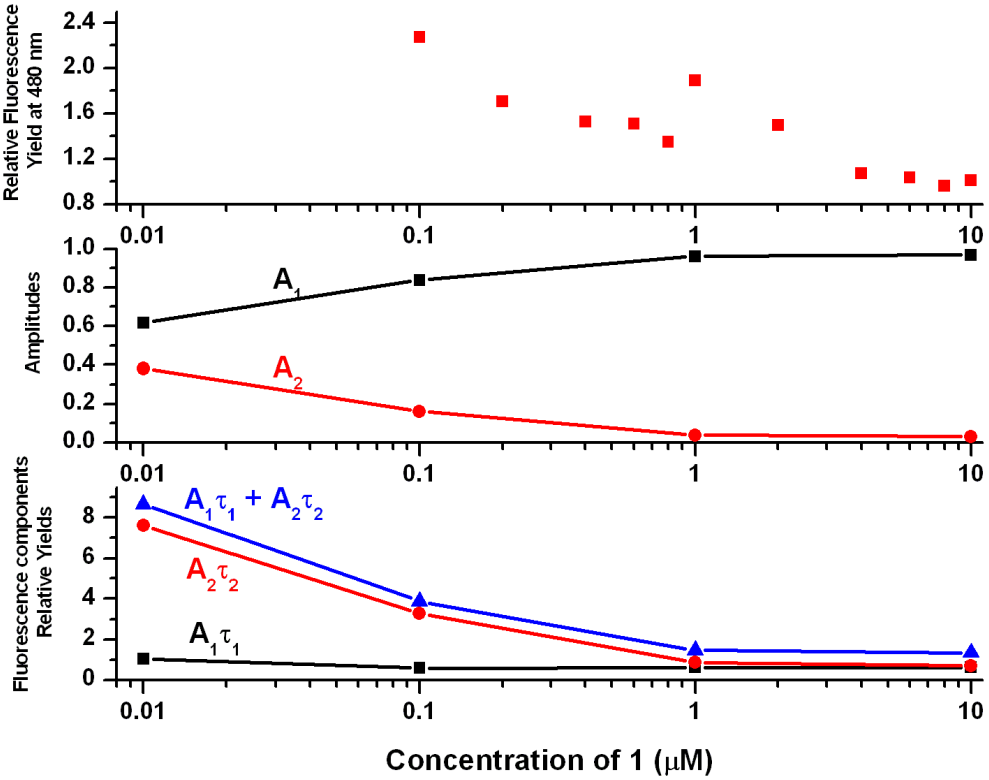

Figure S5. *Top:* Steady-state fluorescence yield (relative units) determined by dividing the observed signal in the emission spectra at 480 nm by the concentration of **1**. *Middle:* Fluorescence amplitudes, A_{1f} and A_{2f}, determined from the decay profiles measured at different concentrations of **1** in the absence of Zn**.** *Bottom:* Contributions of the two components determined from the fluorescence decay profiles to the overall fluorescence intensity of **1** at different concentrations in the absence of Zn. Note the excellent correlation between the relative yields determined from the steady-state fluorescence spectra (top) and the time-resolved spectra ($A_{1}\tau_{1f} + A_{2f}\tau_{2f}$, bottom) in the concentration range of **1** from 0.1 to 10 μM. The subscripts *f* have been left out within the figures.

The fluorescence yield of **1** in aqueous buffer solution (0.1 M KNO_3, 50 mM HEPES, pH 7.0, 25 ^{o}C) depends markedly on its concentration in the 10 nM to 1 μM range (Figure S5, top). As the concentration of **1** is increased from 10 nM to 1 μM, the fluorescence yield decreases by a factor of ~ 2.5, and remains constant in the range of 1 to 10 μM.

We examined the fluorescence decay profiles at four different and representative concentrations of **1** *in the absence of Zn(II)* in order to assess the changes in fluorescence decay times and associated amplitudes in the concentration range of 10 nM to 10 μM (Table S2). The fluorescence decay profiles are well approximated by two fluorescence components as suggested by the χ^2 values in Table S1:

$$I(t) = C' [A_{1f} \exp(-t/\tau_{1f} + A_{2f} \exp(-t/\tau_{2f})] \quad \text{(S1)}$$

The two components have lifetimes of τ_{1f} and τ_{2f} with amplitudes A_{1f} and A_{2f} respectively, and C' is a proportionality constant.

Table S2. Concentration dependence of the fluorescence parameters of **1** in aqueous buffer solution (0.1 M KNO_3, 50 mM HEPES, pH 7.0, 25 ^oC) (Excitation wavelength: 340 nm; viewing wavelength: 480 nm).

Concentration, μM	τ_{1f} (A_{1f})	τ_{2f} (A_{2f})	χ^2
0.01	1.7* (0.62)	19.9 (0.38)	1.10
0.1	0.70 (0.84)	20.4 (0.16)	1.16
1.0	0.64 (0.96)	21.8 (0.039)	1.23
10.0	0.65 (0.97)	22.8 (0.031)	1.21

The data can be interpreted in terms of a short lifetime (0.65 – 1.7 ns) and a longer lifetime (20 – 23 ns). As shown in Figure S5 (*middle*), as the concentration of **1** is increased the amplitude, A_{1f}, of the fast lifetime component increases, while that of the slow component, A_{2f} , decreases. The contributions of each of the two components to the fluorescence yield are proportional to τ_{1f} x A_{1f} and τ_{2f} x A_{2f}, respectively, and are depicted in Figure S5 (*bottom*). The sum is also shown, and it is evident that the slow lifetime component is dominant at the lower concentrations of **1**, and that the contributions of the two components are comparable at the concentrations of 1.0 and 10 μM. The concentration dependence of the relative fluorescence yields deduced from the fluorescence decay profile parameters (Table S2) is in qualitative agreement with the measurements of the steady-state fluorescence yields as a function of concentration (Figure S5 *top*).

In contrast to aqueous buffer solutions, a single exponential fluorescence decay component of **1** is observed in acetonitrile with a characteristic decay time of 14.6 ns. In the same solvent, the fluorescence decay time of the Zn(II) complex of **1** is 25.7 ns, and is also represented by a single exponential (data not shown). In this solvent, the fluorescence yield of the Zn complex is only ~1.8 times greater than that of the free form of **1**.

The dependence of the fluorescence characteristics of **1** on its concentration in aqueous solution (Table S2, Figures S5) is consistent with a formation of aggregated forms of **1**. This association or complex formation of hydrophobic organic molecules in aqueous environments is characteristic of molecules with significant aromatic character and is often an important determinant of reactivities of organic molecules in aqueous solutions (Breslow, R. (1991) "Hydrophobic effects on simple organic reactions in water". *Acc. Chem. Res.* **24**, 159-164).

Our hypothesis is that the aggregated forms of **1** are dominant at micromolar concentrations, and that their contributions to the overall fluorescence are smallest at the lowest concentrations of **1**. As the concentration of **1** increases, the amplitudes of the aggregated forms increase (A_1 in Figure S5), while the fractions of free molecules (A_2) with a long fluorescence decay time, decreases. This model is supported by experiments in which we added progressively larger amounts of DMSO to the aqueous solutions. For example, at a 40:60 ratio of DMSO:H_2O (by volume), the fluorescence decay is more homogeneous with decay parameters τ_{1f} (A_{1f}) = 6.1 ns

(0.720 and τ_{2f} (A_{2f}) = 19.4 ns (0.28). In this solvent mixture, aggregates are still present, although their decay times are presumed to be longer than in water, while that of the longer component is close to the value of the free form in aqueous solution.

Since the fluorescence yields are proportional to the products $\tau_i \times A_i$, the relative contributions of the two components vary with the concentration of **1**. Because the fluorescence decay times of the free-molecule, or non-aggregated forms (component 2) are much longer (~ 20 – 23 ns) than those of the aggregated forms of **1** (0.64 to 1.7 ns) in aqueous solutions, the overall fluorescence yield is dominated by the free component in the concentration range below 1 μM. At the higher concentrations of **1**, the contributions of the two components to the overall fluorescence yield are comparable (Figure S5). The lifetimes of the short component are more variable than the lifetimes of the long component (Table S2), presumably because there are multiple types of aggregates and their nature cannot be defined in detail.

The fluorescence decay profile measurements and the comparable values of $\tau_{2f} \approx \tau_{Zn}$ are consistent with a mechanism in which the formation of complexes of **1** with Zn(II) disrupt the aggregates. The fluorescence lifetimes of these Zn complexes are similar to those of the free complexes (22.5 ns), suggesting that the liganded Zn ion itself does not significantly alter the fluorescence lifetime of **1**.

Calculation of the equilibrium binding constant *K*

The binding equilibrium is defined as usual:

$$Zn(II) + 1 \rightleftarrows [Zn(\mathbf{1})]$$

The equilibrium constant is defined as $K = [Zn(\mathbf{1})]/[Zn(II)][(\mathbf{1})]$, where [Zn(II)] and [(**1**)] are the concentrations of free Zn(II) and (**1**), respectively. With $[Zn(II)]_T$ and $[(\mathbf{1})]_T$ denoting the total concentrations of each component, the value of K is given by:

$$[Zn(\mathbf{1})] = \{1 + K[Zn(II)]_T + K[(\mathbf{1})]_T - [(1 + K[Zn(II)]_T + K[(\mathbf{1})])^2 - 4K[Zn(II)]_T[(\mathbf{1})]_T]^{1/2}\}/2K$$

The solid line in Figure 2 (inset) in the main text is a plot of this equation with $K = 10^9\ M^{-1}$ (or larger) which is consistent with a stoichiometric mode of binding at $Zn(II)]_T$ and $[(\mathbf{1})]_T \sim 10^{-6}$ M.

A

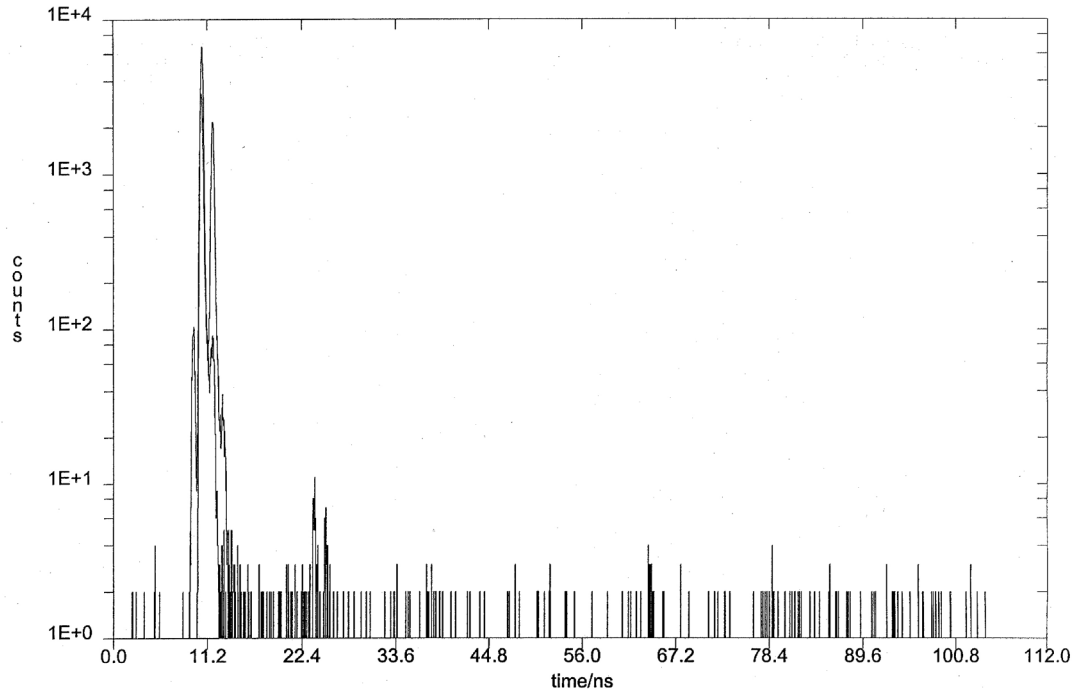

B

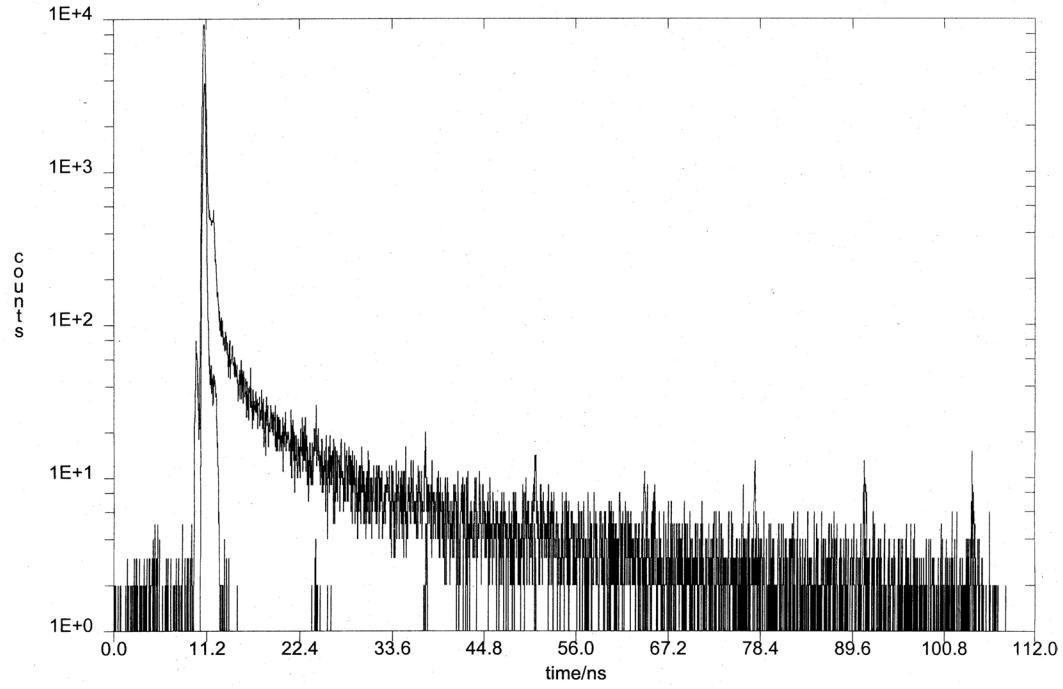

Figure S6. (**A**) Time-resolved fluorescence spectrum of live cells (A549) upon overnight incubation with 20 μM **1** in F12 growth medium. The spectrum was obtained after the dye containing medium was removed and the cells were washed twice with PBS. (B) The spectrum obtained upon treatment with 20 μM zinc pyrithione for 30 minutes and two subsequent washes with PBS.

X-ray Structure of [Zn(1)]

The structure was solved using Bruker SHELXTL[2] and refined using Bruker SHELXTL.[2] The space group P $2_1/c$ was determined based on systematic absences and intensity statistics. A direct-methods solution was calculated which provided most non-hydrogen atoms from the E-map. Full-matrix least squares / difference Fourier cycles were performed which located the remaining non-hydrogen atoms. All non-hydrogen atoms were refined with anisotropic displacement parameters. All hydrogen atoms were placed in ideal positions and refined as riding atoms with relative isotropic displacement parameters. The final full matrix least squares refinement converged to $R1 = 0.0422$ and $wR2 = 0.1155$ (F^2, all data).

The structure was found as a trihydrate with no acetonitrile as a solvate. O11 bridges the cation and anion as a double donor. O12 donates to O11 (in another asymmetric unit) and also lies close to an inversion center. O13 is disordered over two positions a 0.63:037 ratio and donates to both O12 and the ClO_4. The perchlorate anion is disordered over two positions in a 0.63:037 ratio; the perchlorate anion and O13 are tied together for disordered fragments. Only a few protons for the three waters were found in the difference Fourier, but these were enough to place all water protons. Note that the inversion center near O12 forces two protons to be at 50% occupancy. The libration of the primed perchlorate anion is much greater than the unprimed. One of the alkylpyridine ligands (C11-N3) has a degree of librational motion; it was for this reason the data were recollected at 123 K.

[2] SHELXTL V6.14, Bruker Analytical X-Ray Systems, Madison, WI (2000).

Table S3. Crystal data and structure refinement for [Zn(**1**)]

Identification code	05232b	
Empirical formula	C_{26} H_{35} Cl N_6 O_{12} S_2 Zn	
Formula weight	788.54	
Temperature	123(2) K	
Wavelength	0.71073 Å	
Crystal system	Monoclinic	
Space group	$P2_1/c$	
Unit cell dimensions	a = 10.4359(10) Å	α = 90°
	b = 26.531(3) Å	β = 107.108(2)°
	c = 12.5068(12) Å	γ = 90°
Volume	3309.7(6) $Å^3$	
Z	4	
Density (calculated)	1.583 Mg/m^3	
Absorption coefficient	1.019 mm^{-1}	
F(000)	1632	
Crystal color, morphology	Colorless, Block	
Crystal size	0.35 x 0.32 x 0.24 mm^3	
Theta range for data collection	1.54 to 27.52°	
Index ranges	$-13 \le h \le 12$, $0 \le k \le 34$, $0 \le l \le 16$	
Reflections collected	30038	
Independent reflections	7509 [R(int) = 0.0300]	
Observed reflections	6154	
Completeness to theta = 27.52°	98.5%	
Absorption correction	Multi-scan	
Max. and min. transmission	0.7920 and 0.7169	
Refinement method	Full-matrix least-squares on F^2	
Data / restraints / parameters	7509 / 82 / 486	
Goodness-of-fit on F^2	1.079	
Final R indices [I>2sigma(I)]	R1 = 0.0422, wR2 = 0.1061	
R indices (all data)	R1 = 0.0563, wR2 = 0.1155	
Largest diff. peak and hole	0.813 and -0.558 e.$Å^{-3}$	